doi:10.1016/j.jmb.2009.01.037 J. Mol. Biol. (2009) 387, 502–517

JMB

Available online at www.sciencedirect.com

ScienceDirect

ELSEVIER

Statics of the Ribosomal Exit Tunnel: Implications for Cotranslational Peptide Folding, Elongation Regulation, and Antibiotics Binding

Simone Fulle[1] and Holger Gohlke[1,2]*

[1]*Department of Biological Sciences, Molecular Bioinformatics Group, Goethe University, Frankfurt, Germany*

[2]*Department of Mathematics and Natural Sciences, Pharmaceutical Institute, Christian Albrechts University, Kiel, Germany*

Received 8 November 2008; received in revised form 18 January 2009; accepted 21 January 2009
Available online
27 January 2009

A sophisticated interplay between the static properties of the ribosomal exit tunnel and its functional role in cotranslational processes is revealed by constraint counting on topological network representations of large ribosomal subunits from four different organisms. As for the global flexibility characteristics of the subunit, the results demonstrate a conserved stable structural environment of the tunnel. The findings render unlikely that deformations of the tunnel move peptides down the tunnel in an active manner. Furthermore, the stable environment rules out that the tunnel can adapt widely so as to allow tertiary folding of nascent chains. Nevertheless, there are local zones of flexible nucleotides within the tunnel, between the peptidyl transferase center and the tunnel constriction, and at the tunnel exit. These flexible zones strikingly agree with previously identified folding zones. As for cotranslational elongation regulation, flexible residues in the β-hairpin of the ribosomal L22 protein were verified, as suggested previously based on structural results. These results support the hypothesis that L22 can undergo conformational changes that regulate the tunnel voyage of nascent polypeptides. Furthermore, rRNA elements, for which conformational changes have been observed upon interaction of the tunnel wall with a nascent SecM peptide, are less strongly coupled to the subunit core. Sequences of coupled rigid clusters are identified between the tunnel and some of these elements, suggesting signal transmission by a domino-like mechanical coupling. Finally, differences in the flexibility of the glycosidic bonds of bases that form antibiotics-binding crevices within the peptidyl transferase center and the tunnel region are revealed for ribosomal structures from different kingdoms. In order to explain antibiotics selectivity, action, and resistance, according to these results, differences in the degrees of freedom of the binding regions may need to be considered.

Keywords: RNA; flexibility prediction; topological network; ribosomal exit tunnel; cotranslational regulation

Edited by D. E. Draper

Introduction

The ribosome is a large (~2.4 MDa for prokaryotic ribosomes) ribonucleoprotein complex[1] that synthesizes proteins in all kingdoms of life by translating genetic information encoded in mRNA into the amino acid sequence of a protein. The peptide bond is formed at the peptidyl transferase center (PTC) of the large ribosomal subunit. The nascent chain then leaves the ribosome via the ribosomal exit tunnel, which spans the entire large subunit of the ribosome (Fig. 1a).[2] Given a mainly nonsticking Teflon-like character of the tunnel surface, it has been assumed that the tunnel is a passive element of the ribosome that does not interact with the nascent chain.[2] Recent results demonstrate, however, that it does play an active role. It is a key player in cotranslational protein folding processes,[3–5] responds to cellular conditions (which can cause elongation arrest),[6,7] and is a target for clinically relevant antibiotics.[7–17] These findings agree with studies

*Corresponding author. E-mail address: gohlke@pharmazie.uni-kiel.de.

Abbreviations used: PTC, peptidyl transferase center; PDB, Protein Data Bank; cryo-EM, cryo-electron microscopy.

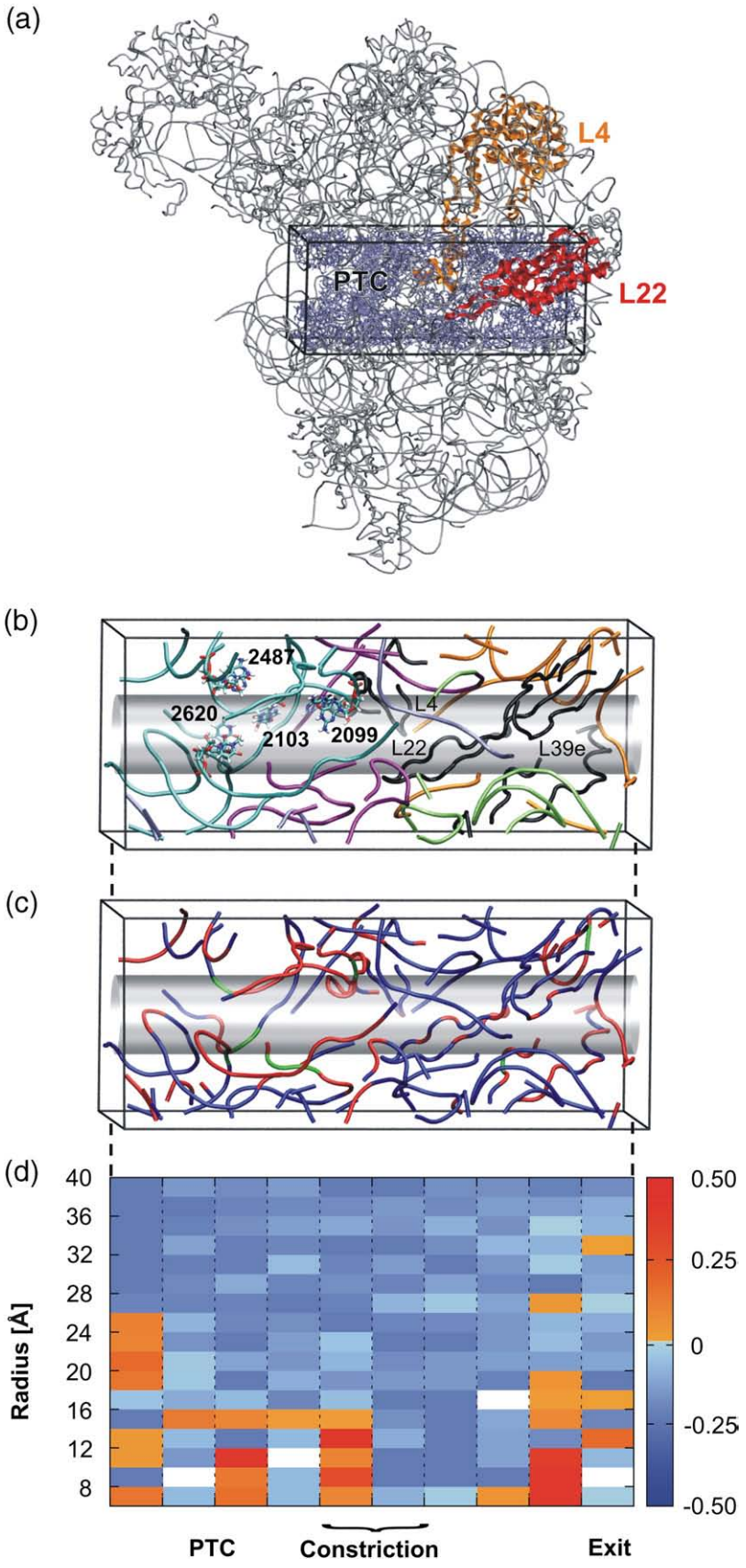

Fig. 1. Global flexibility characteristics of the ribosomal exit tunnel. (a) The atomic structure of the *H. marismortui* 50S ribosomal subunit (PDB code 1S72). Nucleotides and amino acid residues in the neighborhood of the tunnel within an orthorhombus of dimensions 40 Å×40 Å×100 Å are shown in blue. The narrowest constriction of the tunnel is formed by the proteins L4 and L22, which are highlighted in orange and red, respectively. (b) Structure of the 23S RNA within the tunnel region, indicating domain I (orange), domain II (purple), domain III (lime), domain IV (ice blue), and domain V (turquoise). The protein components of the tunnel wall (L4, L22, and L39e) are shown in black. Nucleotides that form the two known antibiotics-binding crevices [nucleotides A2486/C2487 (A2451/C2452EC) and G2099/A2100 (A2058/A2059EC)] and the two potential crevices proposed in this study [nucleotides A2103/C2104 (A2062/A2063EC) and UR3-2619/U2620 (U2584/U2585EC)] are shown in stick representation. A cylinder with a diameter of 15 Å (the average diameter of the tunnel[2]) is shown along the tunnel axis. (c) Color-coded representation of the flexibility characteristics of the tunnel. The coloring of the backbone atoms of the RNA part is performed according to the flexibility characteristics of the P atoms and according to the C^{α} atoms in the protein part. Blue indicates overconstrained regions, red indicates flexible regions, and green indicates isostatically rigid regions. (d) Representation of the flexibility characteristics of the tunnel vicinity in terms of spatial segments. The tunnel region was split into cylindrical shells 10 Å in length, parallel with the tunnel axis (abscissa), and 2 Å in width, perpendicular to the tunnel axis (ordinate). The color-coded representation of the shells is determined by averaging the flexibility indices (Eq. (1)) of P and C^{α} atoms located within a shell. Stable regions are indicated by a color gradient ranging from blue ($f_i=-0.5$) to light blue ($f_i=0.0$); for flexible regions, the gradient ranges from orange ($f_i>0.0$) to red ($f_i=0.5$).

showing that the ribosome behaves in a highly dynamic fashion.[7,18–23] Mainly structural studies of the ribosome have contributed to our understanding of the functional role of the ribosomal exit tunnel.[7,24,25] For example, observed changes in tunnel shape have been implicated to actively promote the passage of

nascent chains[26] or allow for the formation of a compacted peptide chain inside the tunnel.[3,4] Information about the tunnel's role has thus been inferred from conformational changes so far observed between different ribosome states. However, structural studies do not directly probe the static and dynamic properties of a molecule. Here, we apply a computational approach to bridge this gap.

The objective of this work is to investigate the static properties (see below) of the ribosomal exit tunnel based on high-resolution structures of the large ribosomal subunit.[27–30] This is expected to provide a deeper understanding of the active role of the tunnel in cotranslational processes such as peptide folding, elongation regulation, and antibiotics binding. As these processes strongly depend on the local characteristics of the molecular structure, information at the atomic level is required. This precludes an elastic network normal-mode analysis based on a coarse-grained ribosome representation.[20,31,32] As an alternative, molecular dynamics simulations can provide insights in atomic detail,[21] but are still computationally intensive for large assemblies (i.e., require months of computational time to sufficiently sample the conformational space of large assemblies such as the ribosome).[33] Instead, we approach the goal by analyzing static properties (i.e., flexibility and rigidity) of the ribosomal exit tunnel using concepts grounded on rigidity theory (constraint counting).[34–36]

In this context, flexibility determines the possibility of motion within a region (i.e., the region can be deformed). In contrast, no relative motion is allowed within rigid (structurally stable) regions. Rigid regions can only move as a rigid body with six degrees of freedom. Finding flexible and rigid regions is rather like examining a construction and identifying parts that are likely to move (statics), although no information is revealed about the direction and amplitude of the possible motions (dynamics). For constraint counting, a directed graph of covalent and noncovalent constraints within a biomacromolecule is generated from a full atomic representation of the structure.[35] The *pebble game*,[37] a fast combinatorial algorithm, is then applied to exactly enumerate the number and spatial distribution of bond-rotational degrees of freedom in the network. This yields a decomposition of the network into rigid (structurally stable) regions and flexible links. Rigidity within the topological network results from a collection of interlocked bonds in which no relative motion can be achieved without a high cost in energy. If a rigid cluster does not contain redundant constraints, it is isostatically rigid. Conversely, if a rigid cluster contains redundant constraints, it is overconstrained. Finally, underconstrained regions are flexible links between rigid clusters in which the dihedral rotation of bonds is not locked in by other bonds.

Constraint counting has been proven valuable to analyzing the flexibility of proteins[35,38,39] and as a front end for coarse-grained geometric simulations of proteins.[32,40,41] For RNA, we have recently developed a novel network parameterization that reliably captures the flexibility characteristics of these biomolecules.[42]

Constraint counting has already been applied to analyze the global flexibility characteristics of ribosomal subunits.[31] In the present study, we will focus on the local flexibility characteristics of the ribosomal exit tunnel. For this, we analyzed high-resolution structures of large ribosomal subunits of four different species. The large ribosomal subunits of *Haloarcula marismortui* and *Deinococcus radiodurans* have been obtained from crystal structures of isolated 50S subunits [Protein Data Bank (PDB) codes 1S72[27] (2.4 Å) and 2ZJR[30] (2.9 Å)] and are here named H50S and D50S, respectively. The large ribosomal subunits of *Escherichia coli* and *Thermus thermophilus* are here named E50S* and T50S*, respectively, to reflect the fact that they have been extracted from crystal structures containing assembled 70S ribosomes [PDB codes 2AW4[28] (3.5 Å) and 2J01[29] (2.8 Å)]. The crystal structure of the *T. thermophilus* ribosome also contains mRNA and tRNA molecules.[29] These substrates were not considered in the present analysis either. As we included in our analyses structures of unbound isolated large ribosomal subunits alongside structures of the entire ribosome at different functional states, there is a possibility of conformational differences in several ribosome locations and, in particular, the PTC,[28,29,43] as discussed in more detail below. Overall, the ribosomal exit tunnel shows the same size and shape in isolated 50S subunits and assembled 70S ribosomes at different functional states.[44]

The computed flexibility characteristics, in general, display a remarkable level of conservation across species of different kingdoms and a sophisticated interplay between structural stability and function of the tunnel, which corroborates its active role in cotranslational processes.

Results and Discussion

Global flexibility characteristics of the ribosomal exit tunnel

Large parts of the tunnel surface are formed by domains I through V of the 23S rRNA,[45] with significant contributions also made by the ribosomal proteins L4, L22, and L39e in the H50S structure (Fig. 1b).[2,46] L39e replaces the extended tail of L23 found in eubacteria, which do not contain L39e.[43] In all species, the tunnel is largely straight in the second half towards the exit, but has several bends before. For the analysis, the tunnel axis has been oriented such that it is located at the center of the tunnel entrance and tunnel exit regions, respectively, and, defined that way, measures 80 Å in length. The orthorhombus region shown in Fig. 1 has a dimension of 40 Å×40 Å×100 Å and covers, in addition to the tunnel region, also the PTC.

In what follows, the focus of the presentation and discussion of the flexibility characteristics of the ribosomal exit tunnel is based on results obtained for the H50S structure, which shows the highest resolution among all four large subunit structures investigated here. In addition, we compare these results to those obtained for D50S, E50S*, and T50S* in order to determine the level of conservation of the tunnel statics across different species.

Constraint counting on the H50S structure classifies most of the nucleotides and amino acid residues within 20 Å of the tunnel axis to be rigid or overconstrained (Fig. 1c), based on the flexibility indices obtained for phosphorous and C^{α} atoms in the backbone regions. This result also holds true for the rRNA component if the flexibility characteristics of the glycosidic bonds are considered instead (see Fig. S1 in Supplementary Information). Stable regions in the tunnel vicinity can still be identified even if constraint counting is performed on a network in which ~70% of all hydrogen bonds have been deleted, demonstrating the robustness of the analysis (see Fig. S2 in Supplementary Information).

The finding of a stable structural environment of the ribosomal exit tunnel agrees with experimental observations. First, the tunnel does not differ in size and shape when comparing ribosome crystal structures of different species (*H. marismortui*, *D. radiodurans*, *E. coli*, and *T. thermophilus*)[23,27–30,43,44] or substrate analogue and antibiotic complexes.[26] Second, an L22 deletion mutant in H50S does not change the backbone positions of the RNA, although the tunnel expands from ~10 Å to ~19 Å in the region where L4 and L22 come together.[47] Third, significant conformational changes of the ribosomal tunnel are unlikely, as they require the disruption of a very large number of tertiary interactions in the middle of the large macromolecular structure.[44]

In spite of the overall rigidity, there are local zones of flexible nucleotides/amino acid residues within the tunnel (Fig. 1c and d). From the PTC end to the constriction formed by L4 and L22, the nucleotides of domains II and V and the tip of L4 are found to be primarily flexible. Strikingly, local zones of flexibility correspond to backbone regions of domain V comprising the PTC and the entrance of the tunnel, which are main targets for antibiotics binding.[8,47–50] In contrast, the tunnel-wall-forming nucleotides of the last half of the tunnel from domains I, III, and IV and residues of the proteins L4 and L22 are mostly rigid. Only a small group of residues at the tunnel exit is identified as flexible. It is comprised of L39e, as well as flexible nucleotides of domain I.

Notably, a qualitatively very similar flexibility pattern is obtained for the tunnel vicinity of the D50S, E50S*, and T50S* structures (Fig. S3 in Supplementary Information). As in the case of the H50S structure, large parts of the tunnel neighboring region are found to be rigid, whereas clusters of flexible tunnel components are located at the PTC and the tunnel entrance, at the constriction point, and around the tunnel exit.

Implications for the transport of nascent peptide chain and peptide folding

The above results have implications on two intriguing questions: (i) Does the ribosomal tunnel dynamically promote the passage of the nascent peptide chain or does it act as a passive tube? (ii) To what degree can proteins fold in the tunnel? To accommodate a folding polypeptide, the diameter of the tunnel would have to expand by 10–20 Å.[51] The primarily rigid character of the tunnel renders such large-scale conformational changes within the tunnel vicinity impossible, particularly at the center of the tunnel region directly behind the most constricted region. Furthermore, it is questionable whether deformations of the first half of the tunnel will provide a large-enough driving force to promote the entire peptide voyage and, hence, move peptides down the tunnel in an active manner. Thus, the observed structural stability is more consistent with a transport of nascent polypeptides by passive diffusion.[26]

A number of experimental studies have suggested the possibility of secondary structure formation inside the ribosomal tunnel.[3,4,52,53] The diameter of the tunnel varies between 10 Å and 20 Å,[2] which is just enough to allow the formation of an α-helix in the entire tunnel region, provided some bends in the helix axis are permitted.[44] Accordingly, experimental data support the presence of nascent peptides in α-helical conformation.[4] It has been further suggested that nascent peptide chains may adopt some tertiary structure within the tunnel.[3] From a geometrical point of view based on a static picture of the tunnel, this suggestion appears to be unlikely: the largest sphere that can fit inside the tunnel is 13.7 Å, much smaller than the diameter of small protein domains.[44] Yet, a cryo-electron microscopy (cryo-EM) study by Gilbert *et al.* of a translating *E. coli* ribosome showed dynamic walls of the tunnel in the vicinity of the L4 protein.[3] A side pocket of the tunnel opened adjacent to L4, which can accommodate a peptide of ~45 amino acids.[5] This observation raised the question as to whether the tunnel can conformationally adapt to allow for tertiary folding.

According to the constraint counting analysis of H50S, we can rule out this possibility. Although we have identified nucleotides A882/U883 (A789/U790EC), A886/G887 (A793/A794EC) [forming two hinges that allow nucleotides C884/G885 (C791/A792EC) to move], and U1359/C1360 (U1255/G1256EC) adjacent to L4 as flexible (Fig. 2a), allowing for the observed pocket opening, these nucleotides are surrounded by structurally stable regions that make large conformational changes impossible. Convincingly, we will arrive at the same conclusion if the lower-resolution E50S* structure is analyzed instead, which comes from the same organism as investigated in the study of Gilbert *et al.* (Fig. S4 in Supplementary Information).[3]

In any case, we note that the partial folding of the polypeptide suggested by Gilbert *et al.* would occur

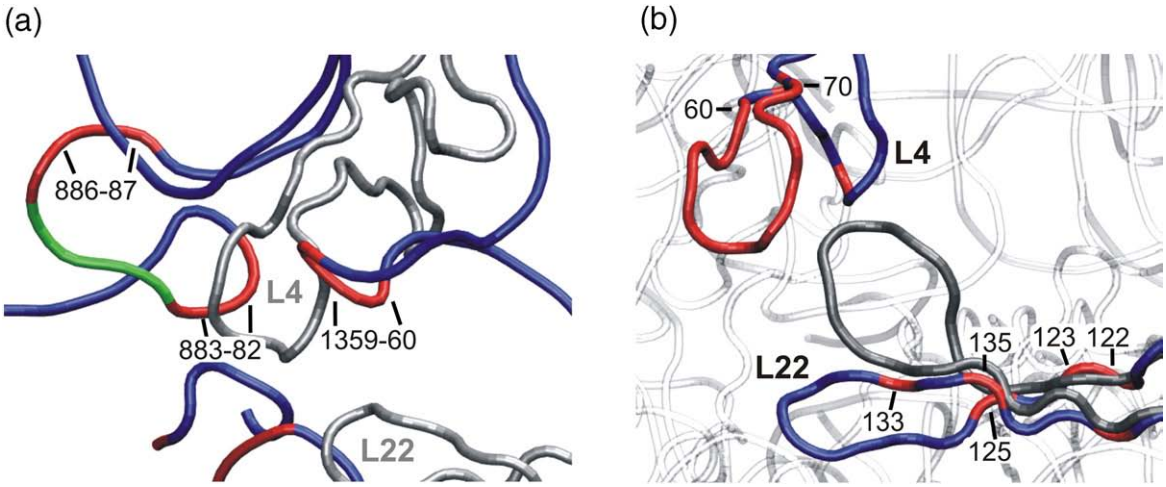

Fig. 2. Flexibility characteristics of the tunnel constriction formed by the ribosomal proteins L4 and L22. Overconstrained regions are indicated in blue, flexible regions are shown in red, and isostatically rigid regions are depicted in green. (a) Flexibility characteristics of nucleotides adjacent to L4. Here, the opening of a side pocket was observed based on cryo-EM.[3] Notably, nucleotides A882/U883 (A789/U790EC) and A886/G887 (A793/A794EC) adjacent to L4 are identified by constraint counting to be flexible, allowing for movements of the enclosed loop. The structural environment of the loop is rigid. (b) Flexibility characteristics of the tunnel-constriction-forming proteins L4 and L22. The coloring of the backbone of the tips of L4 and L22 is shown according to the values of the C^{α} atoms. In addition, the swung conformation of L22 (extracted from PDB code 1OND after superimposition of the L22 structures) is shown in silver.

in the first half of the tunnel. The partially folded peptide must then pass the narrow and largely rigid second half, where moving tunnel walls to provide space for the compact chain appear even less likely. Thus, for traversing this region, the partially folded nascent chain would need to alter its conformation or unfold again.

Recent computational studies of α-helix and β-hairpin formation inside a cylindrical tunnel demonstrate that the folded state is entropically stabilized in the confined compartment.[53,54] In both cases, the diameter of the tunnel was found to be a crucial parameter of secondary structure stability, with critical diameter D_c values of ~8.3 Å[53] and ~13.7 Å,[54] comparable to the dimensions of the ribosomal tunnel. Importantly, it was argued that D_c should depend on the specific peptide inside the tunnel such that cotranslational folding is not universal.[54] Conversely, one would expect that cotranslational folding preferentially occurs in those regions of the tunnel that can conformationally adapt to some extent to provide the optimal D_c for the specific peptide in question. These so-called "folding zones" within the ribosomal tunnel have been identified recently, with the most preferred ones ranging from the PTC to about half of the tunnel, as well as being located at the tunnel exit.[52] Intriguingly, these regions correspond with areas that have flexible tunnel-wall-forming nucleotides or amino acid residues according to the constraint counting (see above and Fig. 1d). This striking agreement between tunnel regions of low structural stability (where an adaptation of the tunnel diameter is likely) and observed folding zones implies that, indeed, compact structures may be stabilized entropically there. In these regions, the tunnel is able to adapt to an optimal diameter and thus can provide a confined compartment that favors structure formation.

Implications for cotranslational elongation regulation and signal transmission to cell components

Constraint counting also provides important insights into the active role of tunnel components in cotranslational elongation regulation. Experimental evidence suggests that certain nascent peptide chains can interact with the tunnel, thereby stalling translation elongation.[55] A striking example is the SecM peptide.[56] A solely mechanical obstruction of the ribosomal exit tunnel due to a folded SecM conformation that plugs the tunnel appears unlikely.[6,57] Instead, translational arrest may arise from a choreographed signaling process between the nascent polypeptide chain and ribosomal components. Several models have been proposed to explain how the constriction point in the tunnel (formed by L22 and L4) is involved in this arrest.[7,25,57,58] Analysis of an L4 mutant strain did not show any apparent involvement of L4 in SecM-mediated stalling,[57,59] while studies of L22 mutant strains demonstrate this protein's active role.[6,57]

Constraint counting on the H50S structure reveals flexibility in residues Arg125 (Ile85EC) and Ala133 (Ala93EC) of the β-hairpin tip of L22 (Fig. 2b). The identified flexible residues in L22 lie at the center of two hinge regions between residues Arg105-Ile107 and Ser113-Asn115 [*D. radiodurans* numbering, which is equivalent to residues Gly124-Lys126 (Arg84-Met86EC) and Arg132-Ser134 (Arg92-Asp94EC) in *H. marismortui* (*E. coli*) numbering].

These molecular hinges have been inferred from an observed conformational change in L22 upon binding of troleandomycin in the ribosomal exit tunnel of *D. radiodurans*.[7] The hinges are also observed when comparing the *isolated* L22 structure[60] to the ribosome-bound conformations of L22[7] (see Fig. S5 in Supplementary Information). Finally, Ala133 (Ala93EC) has been determined to be one of two hot spots for arrest-suppressing mutations in L22.[6]

Apart from the above hinges, the remaining L22 tip is found to be overconstrained when aligned to the tunnel wall. In turn, the tip of the *isolated* L22[60] is found to be flexible throughout (data not shown). Thus, only the pivots around which the tip moves remain flexible for the ribosome-bound L22. This leads to a picture of L22 function in which the L22 tip in its native or swung conformation (no flexibility analysis is possible in the latter case due to missing atomic coordinates of side chains) is rigidified by interactions with the tunnel wall. In fact, in the case of *D. radiodurans*, residues Arg128 (Arg88EC) and Met130 (Lys90EC) have been identified to act as "double hook" for this.[7] One of the two structurally stable conformations of L22 then effectively blocks the tunnel. In between, movement of the tip around the hinges and structural adaptation to the details of the tunnel wall are facilitated by the flexible tip character. Remarkably, exactly the same flexibility pattern is obtained for the L22 β-hairpin of the T50S* structure (Fig. S6 in Supplementary Information), and at least one hinge region is identified in the case of the D50S and E50S* structures (located at Ser92/Arg92EC). Overall, our results support the hypothesis that L22 can undergo conformational changes by either blocking the tunnel in the swung conformation[7] or resulting in further changes in the status of the ribosome[57] (see below). Apparently, L22 can act as a gatekeeper for the voyage of specific peptides.

In contrast, the tip of L4 [Ser60-Val70HM (Trp60-Ser70EC)] is identified to be primarily flexible in all four tested structures (Fig. 2; Fig. S6 in Supplementary Information). Thus, although conformational changes of L4 into the tunnel lumen are possible, a blockade of the tunnel by itself appears unlikely as the tip does not have a stable gate-like character. Interestingly, Crb^{CmlA}-mediated stalling is affected by alterations in the L4 protein, but not by mutations altering L22.[59] As another difference between the two stalling peptides, Crb^{CmlA}-mediated stalling requires a coinducer, chloramphenicol. Chloramphenicol has been suggested to bind differently to the ribosome in this case compared to the binding mode that leads to a general inhibition of protein synthesis. It has thus been proposed that chloramphenicol-induced alterations in the ribosome structure must be combined with Crb^{CmlA}-induced changes in order to establish stalling.[59] Together with our constraint counting results for the tip of L4, one might propose that chloramphenicol-induced alterations in the ribosome structure involve L4, thereby providing a structurally stable tip that can act as a gatekeeper as in the L22 case.

Based on cryo-EM-derived models of a pretranslocational and SecM-stalled *E. coli* ribosome complex, Mitra *et al.* recently proposed a cascade of RNA rearrangements.[25] They propagate from SecM-induced conformational changes of 23S rRNA bases G2099 and C842-A846 (A2058EC and A749-A753EC) in the ribosomal exit tunnel through the large ribosomal subunit, influence the small subunit, and lead to elongation arrest. Morphological and functionally important elements for which significant conformational changes could be observed are the L1 and L7/12 stalks, the GTPase-associated center and the Sarcin-rich loop (SRL), the PTC, the geometry of the intersubunit bridges (IB), and the positioning of tRNAs in all three sites.

When analyzed with the default network parameterization, most of these structural regions are part of the largest rigid cluster, which would not allow for their independent movements (Fig. 3a). However, within a rigid cluster, a hierarchy of regions of varying stabilities can exist.[39,61] In order to reveal such a hierarchy and to investigate whether the cascade of observed rRNA rearrangements is transmitted from the tunnel vicinity through the large ribosomal subunit via regions of varying structural stabilities, we reanalyzed network representations of the subunit with reduced numbers of hydrogen bonds. Hydrogen bonds were removed successively with decreasing E_{HB}, which simulates a melting of the network and results in a hierarchy of regions of varying stabilities.[39]

With the exception of the intersubunit bridge B1a, all of the abovementioned elements involved in rRNA rearrangements rapidly peel off the large rigid core of the subunit and form rigid clusters by themselves. So, too, does the central protuberance, in agreement with its highly mobile character[19] (Fig. 3a). This demonstrates that those elements for which significant conformational changes have been observed experimentally are only weakly coupled to the large ribosomal subunit core. The highly stable character of B1a identified here is consistent with a study by Gao *et al.*, according to which the RNA side of B1a remains quite static even upon the ratchet-like motion of the two subunits.[19]

The analysis furthermore reveals that, for some of the proposed rearrangements, information may be transmitted through structurally stable regions from induced conformational changes within the tunnel. This holds true for bases that constitute, in part, the PTC in the central loop in domain V, as well as for helices 68, 69, and 71 forming the intersubunit bridges B2a–B2b, B3, B5, and B7a, and the sites for the tRNAs.[19] In both cases, a direct sequence of rigid clusters from the tunnel region is found (Fig. 3b); these clusters segregate early from the large rigid core upon network dilution. In the case of the PTC, a conformational change in the nucleotide G2099 (A2058EC) is transmitted via small rigid clusters containing 23S rRNA bases A2100, A2103/A2538, G2102, and A2485/C2536 (A2059, A2062/A2503, G2061, and A2450/C2501 EC). In the second case, the information is initially transmitted via small

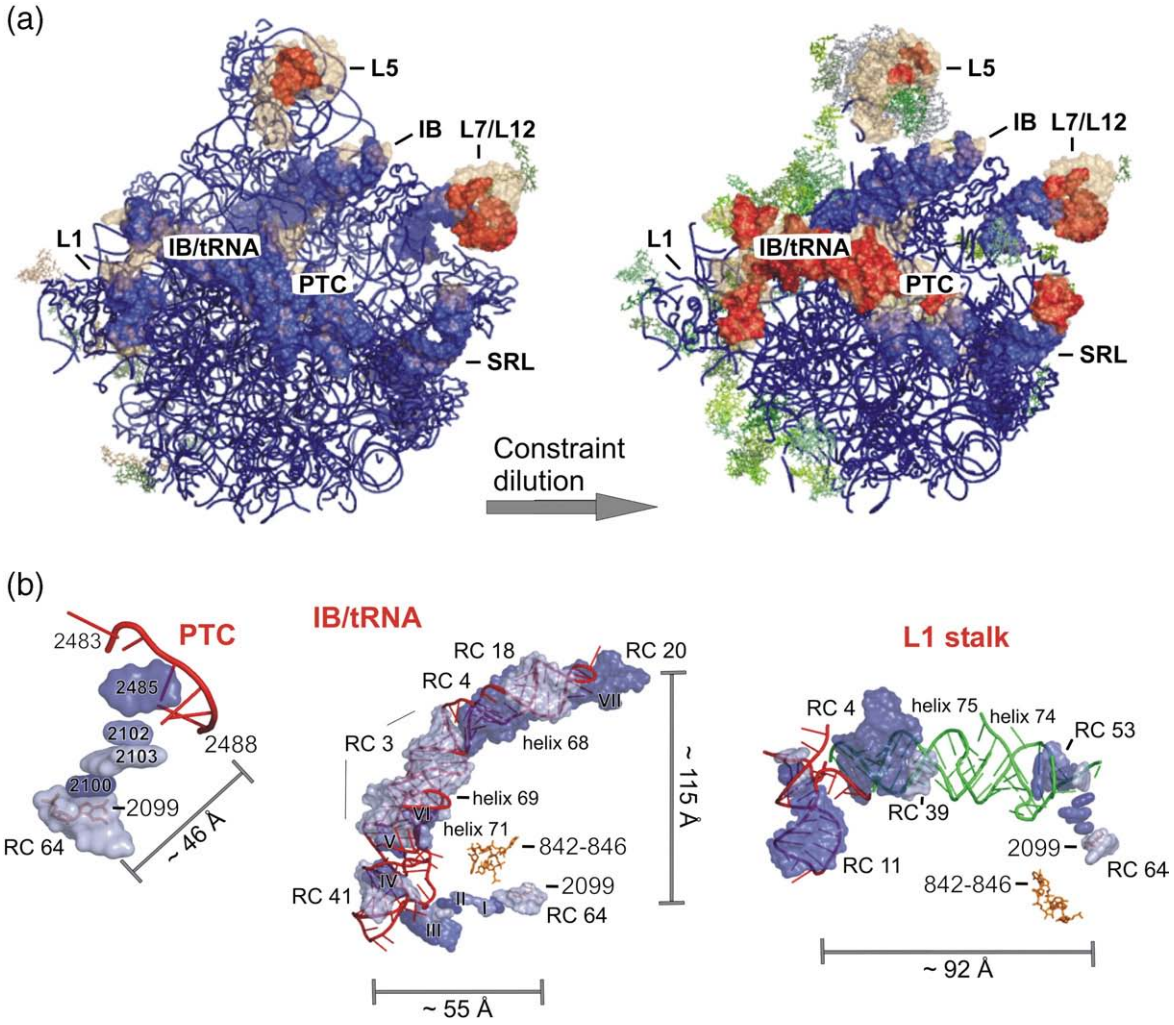

Fig. 3. Signal transmission from the ribosomal exit tunnel that leads to elongation arrest. The SecM nascent polypeptide causes elongation arrest while interacting with 23S rRNA bases G2099 and C842-A846 (A2058EC and A749-A753EC) in the tunnel wall. (a) The largest rigid cluster is represented by a blue backbone representation. Regions for which significant conformational changes are observed in a SecM-stalled ribosome relative to a prestate ribosome complex[25] are shown in a surface representation. Experimentally determined mobile regions that are part of the largest rigid cluster are shown in blue; mobile regions that form separate rigid clusters are shown in reddish hues. Other rigid clusters with at least 50 atoms are shown in greenish hues. Left: The underlying network representation is based on $E_{HB} = -0.6$ kcal/mol (-1.0 kcal/mol) for protein (RNA). Right: The underlying network representation is obtained by diluting the H-bond network (i.e., $E_{HB} = -2.4$ kcal/mol for protein and RNA). (b) Signal transmission occurs through structurally stable regions (depicted in surface representation with bluish hues) starting from the induced conformational change within the tunnel (orange) to the PTC (left), the tRNA region (middle), and the L1 stalk (right) (red cartoon representation). In the case of the PTC, the structurally stable region denoted as "2103" contains nucleotides A2103 and A2538, the region denoted as "2485" contains nucleotides A2485 and C2536, whereas nucleotides A2100 and G2102 form their own cluster. In the case of the tRNA region, structurally stable regions are denoted by roman numerals (I: G2540; II: OMG2588 and RC 102/141/269; III: RC 84/136; IV: RC 117/118/161/214/260; V: RC 129/222; VI: RC 86/140; VII: RC 159). In the case of the L1 stalk, the signaling pathway proposed by Mitra *et al.* comprises helices 74 and 75 (green cartoon representation).[25]

rigid clusters comprising 23S rRNA bases and nucleotides G2540, OMG2588/U2589, U2541/G2618, OMU2587, U2590/C2591, and U2586/G2592 (G2505, G2553/U2554, U2506/G2583, U2552, U2555/C2556, and C2551/G2557 EC), then mainly via the larger rigid clusters 41, 3, 4, 18, and 20 (cluster numbering according to the size of the rigid cluster in the decomposition), with contributions by the smaller rigid clusters 117/118/161/214/260 (IV in Fig. 3b), 129/222 (V), 86/140 (VI), and 159 (VII).

In contrast, the signal transmission pathway proposed by Mitra *et al.*, which comprises helices 61, 64, 67, 72, and 73, is located, to a large extent, within the largest rigid cluster.[25] Thus, no independent movement of these structural regions seems possible. Overall, our findings suggest that the transmission of conformational changes from the ribosomal exit tunnel to the affected region is based on mechanical coupling between specific structurally stable regions. This leads to a signal propa-

gation that resembles a domino-effect-like transformation, albeit with "dominos" of varying sizes. In the case of the tRNA sites being involved, the signal transmission thereby occurs over a distance of >100 Å.

In the case of the L1 stalk (helices 76–79), a signal transmission from the tunnel vicinity can only partially be explained by a sequence of coupled rigid clusters. Whereas rigid clusters are identified in the neighborhood of nucleotide G2099 (A2058EC) and the L1 stalk, parts of helices 74 and 75 are located within the largest rigid cluster (Fig. 3b). No sequences of coupled rigid clusters that lead to the L7/L12 stalk and the GTPase-associated center (helices 42–44), the intersubunit bridge B1a (helix 38), and the Sarcin-rich loop are found. It cannot be ruled out that methodological limitations preclude the identification of transmission pathways here. Alternatively, not all observed structural rearrangements need to be triggered directly from the ribosomal exit tunnel region. Instead, conformational changes of a morphological entity may also occur indirectly via conformational rearrangements of other entities.

In contrast to the highly conserved L4 and L22, L39e found in H50S is unique to archaea and many eukaryotes.[43] In the bacterial structures D50S, E50S*, and T50S*, the tail of L39e is replaced by an intratunnel loop of L23. The loop penetrates into the same region of the tunnel wall as the tail of L39e, but is less deep.[43] This observation has led to the suggestion that, with an increase in cellular complexity, better control of the tunnel's opening is required; for this, two proteins (L23 and L39e) in H50S replace a single one (L23) in eubacteria.[43]

In eubacteria, the internal loop of L23 reaches the tunnel interior, whereas the globular domain is located at the surface of the ribosomal subunit. There, it functions as a binding site for the trigger factor, a bacterial chaperone, and the signal recognition particle for cotranslational protein sorting.[62–64] One may thus anticipate that the bacterial L23 is responsible for information transmission between cell components and newly synthesized nascent chains, as has been suggested in the signal recognition particle.[65] Furthermore, L23 may interact, via its loop, with nascent chains passing through the tunnel, thereby controlling the departure of peptides at the tunnel exit.[43,66] Our analysis identifies the loop of L23 in T50S* as primarily rigid but possessing some flexible residues around the tip region (Fig. S7 in Supplementary Information). An overall rigid character would be a prerequisite for a mechanical signal transmission as described for the SecM-induced conformational changes described above. In the case of D50S and E50S*, a rather flexible loop of L23, which may be attributed to a lower resolution at least for the E50S* structure, is found.

The loop of L39e of H50S in this region is found to be primarily flexible (Fig. S7 in Supplementary Information). This is in agreement with the observed structural disorder of loop residues in this region. A flexible character is incompatible with a mechanical signal transmission; indeed, L39e is a small protein of an extended conformation that lacks a globular domain at the subunit surface to which the information could be transmitted. In accordance, as for the function of the homologous L39 of yeast, the protein has been found to be important only for subunit assembly and translation accuracy, and mutant cells lacking L39 even remained viable.[67,68] Also in this spirit, L39 has been proposed to act as a latch for a gate formed by a tetraloop at the tip of helix 24 of the 23S rRNA, which then transmits a signal to the PTC region via the nascent chain.[33]

Flexibility characteristics of antibiotics-binding crevices

Clinically important antibiotics specifically inhibit the activity of eubacterial ribosomes by binding to the PTC and the ribosomal tunnel region at adjacent or overlapping sites.[8,69] Extensive crystallographic studies (reviewed by Yonath[70] and Poehlsgaard and Douthwaite[71]) have provided detailed analyses of ribosome–antibiotic interactions. In particular, two binding crevices have been identified: one at the PTC, and the other at the entrance of the ribosomal exit tunnel region,[8,47–50] termed active site crevice and exit tunnel crevice, respectively.[49] Although the active site crevice is not part of the ribosomal exit tunnel, which is the major subject of this study, we decided to include a detailed analysis of its flexibility characteristics given its close proximity to the exit tunnel crevice, which even leads to overlapping binding of specific antibiotics.[8,69] Still, peptide-bond formation at the PTC may require static properties of the active site crevice that are different from the properties of the exit tunnel crevice located in the progression pathway of nascent peptide chains.

For now, we limit our constraint counting analysis to both crevice-forming pairs of adjacent bases [A2486/C2487 (A2451/C2452EC) and G2099/A2100 (A2058/A2059EC), respectively] that splay apart along their minor groove and form a wedge-shaped hydrophobic gap between them. With this, we aim at identifying whether differences in the statics of these major parts of antibiotics-binding sites exist between unbound ribosome structures of different organisms. A more detailed analysis of factors involved in antibiotics binding, action, selectivity, and resistance would also require taking into account energetic measures, extended binding site regions, and analysis of antibiotics-bound ribosome structures. Such an analysis is beyond the scope of the present study.

Constraint counting on H50S reveals a dual-flexibility character for these crevices (Table 1, Fig. 4): in both cases, the glycosidic bond of one of the imperfectly stacked base pairs is flexible [A2486 (A2451EC) and A2100 (A2059EC), respectively], whereas that of the other one is found to be over-constrained or rigid [C2487 (C2452EC) and G2099 (A2058EC), respectively]. The static properties of the backbone of the crevice-forming nucleotides resemble

Table 1. Flexibility characteristics and experimentally determined torsion angles of the antibiotics-binding crevices at the PTC and in the ribosomal exit tunnel

Organism	Nucleotide ID[a]	Flexibility characteristics of glycosidic bonds	Range of torsion angles of glycosidic bonds
H. marismortui	A2486/C2487	Flexible/overconstrained	15.1°/12.5°[b]
	G2099/A2100	Rigid/flexible	11.7°/20.5°[b]
D. radiodurans	A2430/C2431	Overconstrained/overconstrained	17.6°/25.9°[c]
	A2041/A2042	Rigid/flexible	26.6°/32.8°[c]
E. coli	A2451/C2452	Overconstrained/overconstrained	—
	A2058/A2059	Flexible/flexible	
T. thermophilus	A2451/C2452	Overconstrained/overconstrained	—
	A2058/A2059	Flexible/flexible	

[a] Nucleotide numbering refers to the PDB entry of the respective organism.
[b] The range of torsion angles of the glycosidic bonds determined in the crystal structures of unbound H50S, as well as those bound to antibiotics at either of the two antibiotics-binding crevices.
[c] The range of torsion angles of the glycosidic bonds determined in the crystal structures of unbound D50S, as well as those bound to antibiotics at either of the two antibiotics-binding crevices.

the properties of the glycosidic bonds, respectively, except for C2487. That is, the backbones of A2486, C2487, and A2100 are flexible, whereas the backbone of G2099 is found to be rigid. The structural stability of C2487 and G2099 can be explained by the two bases being stacked onto the terminal base pair of an

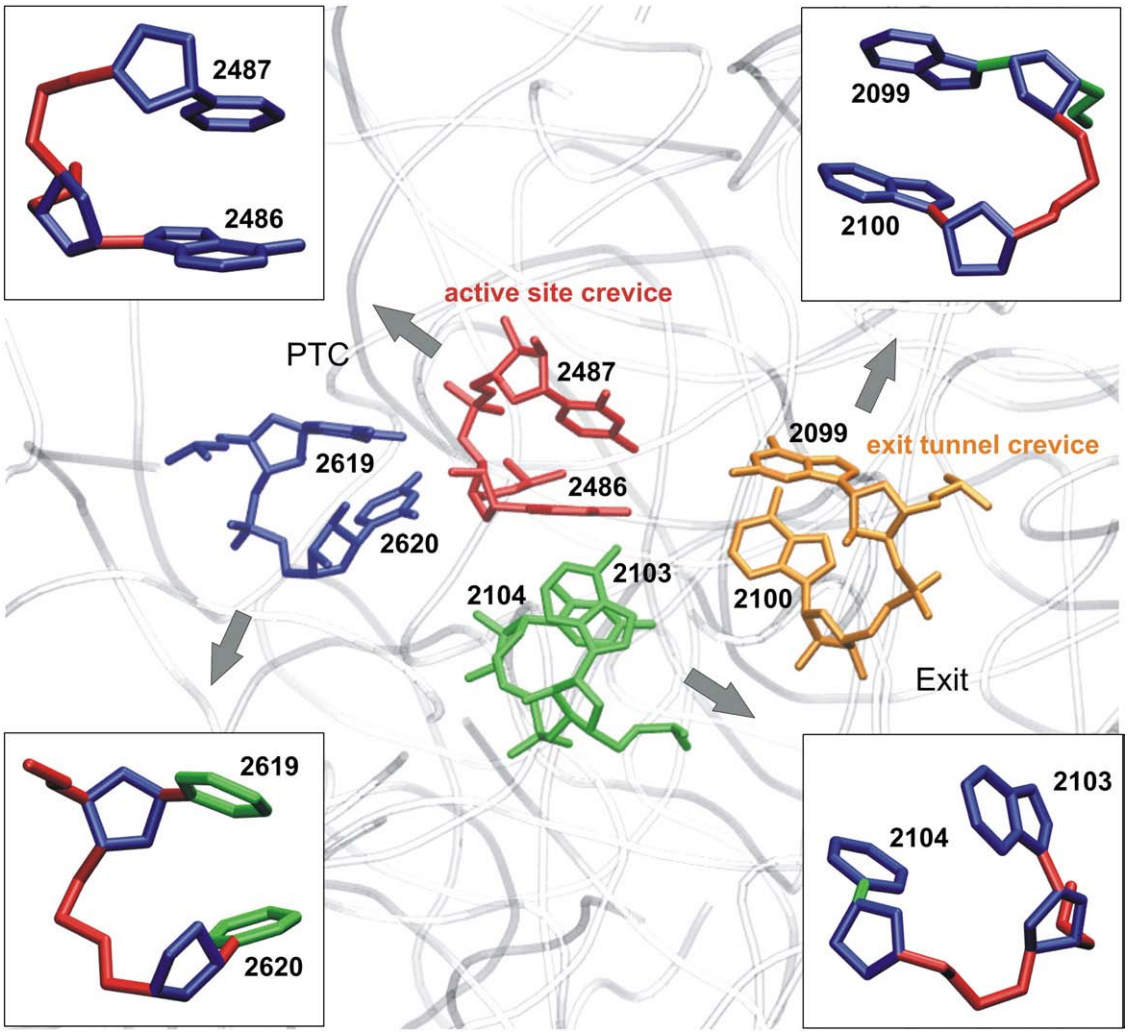

Fig. 4. Flexibility characteristics of binding crevices at the PTC and within the ribosomal exit tunnel. The active site crevice (red) and the crevice formed by the two nucleotides UR3-2619/U2620 (U2584/U2585EC) (blue) are located at the PTC and at the tunnel entrance, on opposite tunnel walls. The exit tunnel crevice (orange) is close to the tip of L4. The crevice formed by nucleotides A2103/C2104 (A2062/A2063EC) (green) is located midway between the other crevices. The flexibility characteristics are indicated in green for isostatically rigid regions, in blue for overconstrained regions, and in red for flexible regions.

adjacent helical region. The findings are also consistent with the range of torsion angles of the glycosidic bonds observed in different ribosome crystal structures of unbound H50S and bound to antibiotics.[16,27,47–49] In the case of the flexible bases, the range amounts to 15.1° (20.5°) for A2486 (A2100), whereas it is only 12.5°/11.7° in the case of both rigid bases (C2487 and G2099).

The flexible bases allow for a conformational variability of the crevices and may explain why antibiotics from different structural classes can be accommodated by one binding site.[49] Furthermore, the dual-flexibility character indicates why an A2099G mutation of the key nucleotide determining macrolide selectivity does not result in significant changes in the binding modes of the antibiotics.[47] The flexible partner base A2100 provides sufficient conformational adaptability for the crevice to accommodate the macrolide at a higher concentration in a geometry that is similar to that of the wild-type ribosome.

We then set out to search for further potential binding sites in the ribosomal exit tunnel of H50S. We required that such a binding site has two sequentially adjacent, imperfectly stacked bases, oriented towards the tunnel lumen, that either allow for conformational adaptation or already provide enough space to accommodate a ligand group via stacking interactions. Identifying unexploited sites opens up considerable opportunities for structure-based design of novel drugs.[71] Surprisingly, although the tunnel wall offers a plethora of indentations that could potentially act as target sites, we were only able to identify two other crevices that fulfill the above criteria.

The first crevice is formed by nucleotides A2103 (A2062EC; flexible) and C2104 (C2063EC; rigid) (Fig. 4). A2103 is located midway between the active site crevice and the exit tunnel crevice and can interact with antibiotics or substrates bound at either crevice.[49] Importantly, A2103 shows pronounced conformational changes of the base depending on whether binding partners are bound at the A-site, bound at the P-site, or not bound at all.[2,72,73] This confirms our prediction of a flexible glycosidic bond. Even more important, binding of virginiamycin M to the active site crevice of H50S[47,49] rotates the base of A2103 by 90° towards the tunnel lumen, so that virginiamycin M also interacts with a second (expanded) crevice formed by A2103 and C2104. In all eubacterial ribosome structures reported so far,[23,28–30,43,74–76] A2103 has been observed only in this repositioned extended conformation.[49] Together with suggestions that A2103 may be critical for stalling[77] and may play an active role in protein biosynthesis,[66] this illustrates that the crevice between A2103 and C2104 may indeed be a valuable target.

The other crevice that also shows two sequentially adjacent, imperfectly stacked bases within the tunnel region is formed by nucleotides UR3-2619 (U2584EC) and U2620 (U2585EC) and is located at the tunnel side opposite to the active site crevice. Here, the backbone and the glycosidic bonds of both nucleotides are identified to be flexible. The highly flexible character is in agreement with dramatic conformational changes of U2620 that have been observed upon binding of an active site substrate[2,72] or virginiamycin M in the H50S case.[49] To the best of our knowledge, no antibiotics binding within this crevice has been described, although, for example, virginiamycin M interacts with the opposite side of U2620.[49] This finding is even more remarkable if one considers that the site is in close proximity to the active site crevice and that the base pairs of both crevices are oriented roughly in parallel with respect to each other. The proposed crevice would thus offer the possibility for antibiotics to simultaneously exploit two hydrophobic binding sites.

Subtle structural differences within the antibiotics-binding pockets of the prokaryotic and eukaryotic ribosomes[78,79] are key to antibiotics selectivity.[70] In this regard, *H. marismortui* ribosomes are distinct from eubacterial ones, as they possess typical eukaryotic elements at the principal antibiotic target sites and require much higher than clinically relevant antibiotics concentrations for binding.[48,49,70,80,81] In order to investigate whether the structural differences are also reflected in the different flexibility characteristics of the antibiotics-binding crevices, we also analyzed the eubacterial D50S, E50S*, and T50S* structures.

Interestingly, a conserved dual-flexibility character of the crevice-forming nucleotides could not be revealed by constraint counting. Instead, we found in all cases that the two glycosidic bonds of the active site crevice nucleotides are predicted to be overconstrained. The two glycosidic bonds of the exit tunnel crevice nucleotides are identified to be flexible in the case of the E50S* and T50S* structures (Table 1); in the case of the exit tunnel crevice forming nucleotides of the D50S structure, a dual-flexibility character could be identified again.

Unfortunately, experimental E50S* or T50S* structures bound to antibiotics at either of the two crevices that could be used for verifying these results, as in the H50S case, are not available. In the case of *D. radiodurans*, unbound 50S ribosomal subunit structures, as well as those bound to antibiotics at either of the two sites,[7,8,11,12,15,30,82] do reveal smaller ranges of adapted glycosidic bond torsion angles for nucleotides with rigid glycosidic bonds [A2041DR, A2430DR, and C2431DR (A2058EC, A2451EC, and C2452EC): 26.6°, 17.6°, and 25.9°] compared to the flexible nucleotide A2042DR (A2059EC) of the exit tunnel crevice (32.8°), supporting our analyses.

Although the resolution of eubacterial structures is lower than that of H50S, it is remarkable that consistent results are found for all three eubacterial cases for the active site crevice, mutually corroborating the analyses. This finding is even more significant if one considers that, in contrast to D50S and E50S*, the T50S* structure is of a functional ribosome where the PTC is partially occupied by substrates. Although conformational differences in the PTCs of all three

structures exist,[28,29] these differences do not give rise to differences in the static properties of the active site crevices.

When comparing the apo crevices of H50S to corresponding clefts of the eubacterial D50S, E50S*, and T50S* structures, a wider active site crevice is found for the latter ones, as is a narrower exit tunnel crevice. This has led to the notion that the active site cleft may always be open in eubacterial ribosomes.[83] Furthermore, it has been hypothesized that this could be the reason that eubacteria are more sensitive to some of the active site crevice antibiotics than archaea: the already open conformation would not require any of the binding free energies expended to accommodate the appropriate bound conformational state.[83] While our constraint counting results do not allow us to draw any conclusions on the energetics of such changes, they are not contradictory to these observations either. In fact, eubacteria would benefit if the open conformation of the active site crevice is structurally stabilized, as given by overconstrained glycosidic bonds of its nucleotides. In turn, the flexible glycosidic bonds of the exit tunnel crevice would allow for more conformational adaptability in the eubacteria case in order to compensate for the narrow apo conformation. We note, however, that the selectivity of PTC antibiotics also can be acquired by means other than crevice "wideness." In the case of pleuromutilins, interactions between nucleotides that do not interact with the bound antibiotics are exploited for selectivity, in a manner resembling allosteric effects.[84]

Conclusions

Flexibility and mobility underlie biological function. This holds true particularly for the ribosome, which undergoes diverse structural changes during the process of protein synthesis. Given the enormous size of the ribosomal complex and given that peptide elongation occurs on the order of seconds,[85] the simulation of translation processes, with biologically relevant time scales, by molecular dynamics simulations is still infeasible. Here, we investigate the function of the ribosomal exit tunnel by analyzing the *static* properties (i.e., flexibility and rigidity) of the large ribosomal subunit using concepts grounded on rigidity theory. These analyses are based on a novel representation of topological networks for RNA-containing structures previously developed in our laboratory.[42] From a methodological point of view, our results demonstrate that, by analyzing ribosome structural stability, a deeper understanding of the exit tunnel's function down to the atomic level can be gained at reasonable computational expenses. From a biological point of view, the analyses provide critical insights into the role of the ribosomal exit tunnel during protein synthesis.

In order to investigate the validity of the constraint counting results across different organisms, we analyze four crystal structures of the large ribosomal subunit from all available different organisms (H50S, D50S, E50S*, and T50S*). The quality of the structures has been found to be important for the accuracy of the flexibility analyses.[35,86] The H50S structure has the highest resolution (2.4 Å) and allows for incorporating resolved metal ions into the constraint counting analysis, whereas the eubacterial structures have lower resolutions (D50S: 2.9 Å; E50S*: 3.5 Å; T50S*: 2.8 Å), and the T50S* structure does not contain metal ions. One might thus expect a lower level of accuracy for the flexibility analyses based on these topological networks. It is therefore all the more reassuring that global flexibility characteristics and local static properties, based on structural features that are conserved across organisms, are generally also conserved. Yet, our analyses also allow identification of differences between flexibility characteristics in those cases where structural differences have already been described to be important for functional differentiation. In more detail, the following results stand out.

First, most parts of the tunnel neighboring regions were identified to be rigid. This holds true for all high-resolution structures of the large ribosomal subunit of different organisms available in the PDB database.[27–30] Even more striking is the finding of conserved local zones of flexible nucleotides/amino acid residues within the tunnel: Clusters of flexible tunnel wall components are located at the PTC, at the constriction point formed by the ribosomal proteins L4 and L22, and around the tunnel exit. Again, these local zones were identified across all four ribosomal subunit structures investigated. Interestingly, these regions correspond to previously identified zones of secondary structure formation within the tunnel.[52] The agreement between tunnel regions with low structural stability and observed folding zones implies that, indeed, secondary structure may be stabilized entropically there through local conformational adaptability of the ribosomal exit tunnel. In contrast, the constraint counting analysis rules out that the tunnel can adapt conformationally to allow for tertiary folding.

Second, based on the first high-resolution structure of the large ribosomal subunit, it has been proposed that an important role of most ribosomal proteins is to stabilize the three-dimensional structure of the rRNA.[46] However, recent experimental data indicate the possibility of conformational changes of the L22 β-hairpin within the tunnel,[7] which have been connected with elongation regulation[7] and folding processes.[4]

For the highly conserved tunnel proteins L4 and L22, the locations of the investigated species (H50S, D50S, E50S*, and T50S*) in the ribosomal tunnels are rather similar. Thus, a conserved role of these tunnel components in regulation appears likely. In agreement, previous experimental findings of hinge regions in the L22 β-hairpin in D50S[7] exactly correspond to flexible residues within the L22 β-hairpin of the H50S and T50S* structures identified

here by constraint counting. In connection with structurally stable parts of the remaining L22 tip when aligned to the tunnel wall, one may assume that one of the two experimentally observed conformations of L22 can effectively block the tunnel. In contrast, the finding of a highly flexible tip of L4 conserved across all investigated structures gives us no hint as to a tunnel-blocking function of this protein *per se*. Rather, we propose that chloramphenicol is required as a coinducer in the case of Crb^{CmlA}-mediated stalling to stabilize the loop so that it can then act as a gatekeeper.

An important related question arises as to how signals triggered by the nascent chain inside the tunnel propagate through the ribosomal structure and influence translation. By determining a hierarchy of regions of varying stabilities of H50S, we were able to identify rRNA elements that are only weakly coupled to the ribosomal subunit core. These elements almost perfectly agree with those that have been identified experimentally to be involved in RNA rearrangements of the *E. coli* ribosome complex and eventually lead to a SecM-induced stalling.[25] Furthermore, for some of the proposed rearrangements, our analysis reveals that information may be transmitted through structurally stable regions from induced conformational changes within the tunnel. In contrast to the signal transmission pathway proposed by Mitra *et al.*, which is located, to a large extent, within the largest rigid cluster of the subunit, our findings suggest an alternative signal transmission by mechanical coupling between specific structurally stable regions, mimicking a domino-like effect rather than a rigid-body transformation of a single region.[25] This arrangement of structurally stable regions is reminiscent of a tensegrity architecture, which consists of a tensed network of structural members that resist shape distortion.[87] This type of architecture particularly suits mechanical signal transmission because a local force, as generated from SecM-induced conformational changes of 23S rRNA bases inside the tunnel, can produce global structural rearrangements.[88,89] Albeit stable, the architecture provides the flexibility necessary to change the shape of an entire structure even at a distance.

Regarding the eubacterial L23, we identified the loop reaching the tunnel interior to be primarily rigid in the case of T50S*. This rigid character would allow for a mechanical signal transmission from an interacting nascent chain to the protein's globular domain, which is located at the surface of the ribosomal subunit and functions as a binding site for other cellular components.[62–64] In contrast, the loop of L39e of H50S is found to be primarily flexible. The flexible character is incompatible with a mechanical signal transmission, in agreement with the lack of a globular domain to which the information could be transmitted and with the protein's role for subunit assembly and translation accuracy.[33,67,68]

Finally, clinically important antibiotics bind to the PTC and the ribosomal tunnel region at adjacent or overlapping sites. As ribosomes from different organisms show a high degree of sequence, structural, and functional conservations, the question as to how antibiotics binding to humans and antibiotics binding to pathogens are different becomes key to therapeutic effectiveness.[70] Here, we aimed at identifying whether differences in the flexibility characteristics of the active site crevice and the exit tunnel crevice exist between unbound ribosome structures of different organisms and whether these differences can be related to antibiotics selectivity. For H50S, which possesses typical eukaryotic elements at the principal antibiotic targets,[48,49,70,80,81] both crevice-forming pairs of adjacent bases show a dual-flexibility characteristic. This is also supported by the analysis of experimentally observed conformational changes of the bases in unbound and antibiotics-bound ribosome structures. In contrast to the H50S structure, but consistent across all three analyzed eubacterial structures, the two glycosidic bonds of the active site crevice bases of D50S, E50S*, and T50S* are found to be overconstrained, whereas the exit tunnel crevice nucleotides are identified to be flexible. Again, the torsion angle ranges of observed movements of these bases lend support to the constraint counting analyses. Thus, subtle structural differences in the antibiotics-binding pockets of the archaeal and eubacterial ribosomes[78,79] bear on characteristic flexibility patterns for the different kingdoms. Although additional factors, such as the energetics of binding, the influences of components of more extended binding site regions, and mechanisms resembling allosteric effects,[84] need to be taken into account for a detailed analysis of antibiotics selectivity, action, and resistance, our findings at least point to the importance of also considering differences in the degrees of freedom of the binding regions, which relates to entropic influences on the binding process. In this spirit, a wider eubacterial apo active site crevice would benefit from structural stabilization as found here, for then no free-energy contribution is required to shape the appropriate bound conformational state.[83]

Materials and Methods

For constraint counting, four static three-dimensional structures of the large ribosomal subunit from *H. marismortui* (PDB code 1S72[27]), *E. coli* (PDB code 2AW4[28]), *T. thermophilus* (PDB code 2J01[29]), and *D. radiodurans* (PDB code 2ZJR[30]) were modeled as so-called bond-bending networks. Unless otherwise stated, the nucleotide and amino acid residue numbering refers to *H. marismortui*, followed by the equivalent *E. coli* numbering† in parentheses. The H50S structure has a resolution of 2.4 Å, which provides enough structural detail to model the constraint network appropriately,[35,86] and allows incorporation of resolved metal ions (known to strongly affect the stability of RNA structures) into the network.[26,90] The other structures are of lower resolution (D50S: 2.9 Å; E50S*: 3.5 Å; T50S*: 2.8 Å) and do not contain metal ions in the case of T50S*. In

† Provided by http://www.riboworld.com/nuctrans/

the case of the 2ZJR structure, ribosomal proteins L33, L34, and L35 have been excluded from the analysis due to missing protein side chains in the crystal structure. To determine the ranges of adapted torsion angles of the glycosidic bonds of antibiotics-binding crevice-forming base pairs, unbound H50S and D50S structures, as well as those bound to antibiotics at either of the two antibiotics-binding crevices at the PTC and in the exit tunnel with a resolution of ≤ 3.5 Å, were analyzed.

For a full atomic representation, missing hydrogen atoms were added by the *tleap* program of the Amber 9 package.[91] Within the networks, vertices (joints) represent atoms, and edges (struts) represent covalent and noncovalent bond constraints, as well as angular constraints. The *pebble game*,[37] a fast combinatorial algorithm, is then applied to determine the number and spatial distribution of bond-rotational degrees of freedom in the network and, hence, the *local* network flexibility and rigidity.

A continuous quantitative measure of the local flexibility/rigidity characteristics is given by the flexibility index f_i defined for each covalent bond i (Eq. (1)):[35]

$$f_i = \begin{cases} \dfrac{F_j}{H_j} & \text{in an underconstrained region} \\ 0 & \text{in an isostatically rigid cluster} \\ -\dfrac{R_k}{C_k} & \text{in an overconstrained region} \end{cases} \quad (1)$$

In underconstrained regions j, f_i relates the number of independent internal degrees of freedom (F_j) to the number of potentially rotatable bonds (H_j); in overconstrained regions k, the number of redundant bonds (R_k) is related to the number of constraints (C_k). The flexibility index ranges from −1 to 1, with negative values in overconstrained regions and positive values in flexible ones. For visualization, flexibility indices of backbone bonds involving phosphorus and C^{α} atoms were averaged and assigned to the respective atom.[38] For further details about rigidity theory and the underlying algorithms, see Jacobs,[34] Jacobs *et al.*,[35] Jacobs and Thorpe,[37] and Whiteley.[92]

Considering that the flexibility of biomacromolecules is largely determined by noncovalent interactions, the outcome of a flexibility analysis is mainly governed by the way hydrophobic interactions, hydrogen bonds, and salt bridges are modeled in the network.[38] Here, different criteria for modeling noncovalent interactions were used for the protein and RNA parts, owing to the fact that protein and RNA structures have different structural features.[42]

Hydrophobic interactions are modeled as bridges of three pseudo atoms between two hydrophobic interactions if their distance is less than the sum of their van der Waals radii (C: 1.7 Å; S: 1.8 Å) plus 0.25 Å[39] (0.15 Å[42]) in the protein (RNA) case. Furthermore, we limit the number of stacking interactions between sequentially adjacent bases to 1 to avoid overly rigid RNA components.[42]

Hydrogen bonds and *salt bridges* are identified according to geometrical and energetic criteria.[35] For the latter, an empirical potential is used.[35] By tuning the energy threshold E_{HB}, the number of hydrogen bonds included can be varied, influencing the flexibility characteristics of the network. For the flexibility analysis, hydrogen bonds are included in the network by setting $E_{HB} = -0.6$ kcal/mol[35] (−1.0 kcal/mol[42]) in the protein (RNA) case. Additional analyses were performed on networks in which hydrogen bonds have been removed successively with decreasing E_{HB}, leading to a diluted bond network. That way, a hierarchy of regions of varying stabilities can be identified in a network.[39] Salt bridges are considered a special case of hydrogen bonds and are treated by a different energy function.[35,38] RNA/protein interface regions were modeled using the parameterization described above for proteins, indicating that these interface regions are strongly stabilized by the formation of hydrogen-bond networks and intermolecular hydrophobic cores.[93] Interactions with Mg^{2+} resolved in the 1S72, 2AW4, and 2ZJR structures were included as covalent bonds with the network.

Acknowledgements

We are grateful to Dr. Julian Chen (Goethe University, Frankfurt, Germany) and Sara Nichols (Yale University, New Haven, CT) for critically reading the manuscript. This work was supported by the DFG (SFB 579; "RNA–ligand interactions"), Goethe University, and Christian Albrechts University (Kiel, Germany). S.F. acknowledges financial support from the Hessian Science Program, the Frankfurt International Graduate School for Science, and the Otto Stern School in Frankfurt. H.G. acknowledges fruitful discussions at the workshop "Dynamics under Constraints II," McGill University's Bellairs Research Institute, Barbados, 2007.

Supplementary Data

Supplementary data associated with this article can be found, in the online version, at doi:10.1016/j.jmb.2009.01.037

References

1. Korostelev, A. & Noller, H. F. (2007). The ribosome in focus: new structures bring new insights. *Trends Biochem. Sci.* **32**, 434–441.
2. Nissen, P., Hansen, J., Ban, N., Moore, P. B. & Steitz, T. A. (2000). The structural basis of ribosome activity in peptide bond synthesis. *Science*, **289**, 920–930.
3. Gilbert, R. J., Fucini, P., Connell, S., Fuller, S. D., Nierhaus, K. H., Robinson, C. V. *et al.* (2004). Three-dimensional structures of translating ribosomes by cryo-EM. *Mol. Cell*, **14**, 57–66.
4. Woolhead, C. A., McCormick, P. J. & Johnson, A. E. (2004). Nascent membrane and secretory proteins differ in FRET-detected folding far inside the ribosome and in their exposure to ribosomal proteins. *Cell*, **116**, 725–736.
5. Etchells, S. & Hartl, U. (2004). The dynamic tunnel. *Nat. Struct. Mol. Biol.* **11**, 391–392.
6. Nakatogawa, H. & Ito, K. (2002). The ribosomal exit tunnel functions as a discriminating gate. *Cell*, **108**, 629–636.
7. Berisio, R., Schluenzen, F., Harms, J., Bashan, A., Auerbach, T., Baram, D. & Yonath, A. (2003). Structural insight into the role of the ribosomal tunnel in cellular regulation. *Nat. Struct. Biol.* **10**, 366–370.
8. Schluenzen, F., Zarivach, R., Harms, J., Bashan, A., Tocilj, A., Albrecht, R. *et al.* (2001). Structural basis for the interaction of antibiotics with the peptidyl transferase centre in eubacteria. *Nature*, **413**, 814–821.

9. Schluenzen, F., Pyetan, E., Fucini, P., Yonath, A. & Harms, J. (2004). Inhibition of peptide bond formation by pleuromutilins: the structure of the 50S ribosomal subunit from *Deinococcus radiodurans* in complex with tiamulin. *Mol. Microbiol.* **54**, 1287–1294.
10. Schluenzen, F., Takemoto, C., Wilson, D., Kaminishi, T., Harms, J., Hanawa-Suetsugu, K. *et al.* (2006). The antibiotic kasugamycin mimics mRNA nucleotides to destabilize tRNA binding and inhibit canonical translation initiation. *Nat. Struct. Mol. Biol.* **13**, 871–878.
11. Harms, J. M., Schlüenzen, F., Fucini, P., Bartels, H. & Yonath, A. (2004). Alterations at the peptidyl transferase centre of the ribosome induced by the synergistic action of the streptogramins dalfopristin and quinupristin. *BMC Biol.* **2**, 4.
12. Berisio, R., Harms, J., Schluenzen, F., Zarivach, R., Hansen, H. A., Fucini, P. & Yonath, A. (2003). Structural insight into the antibiotic action of telithromycin against resistant mutants. *J. Bacteriol.* **185**, 4276–4279.
13. Berisio, R., Corti, N., Pfister, P., Yonath, A. & Böttger, E. C. (2006). 23S rRNA 2058A →G alteration mediates ketolide resistance in combination with deletion in L22. *Antimicrob. Agents Chemother.* **50**, 3816–3823.
14. Pfister, P., Corti, N., Hobbie, S., Bruell, C., Zarivach, R., Yonath, A. & Böttger, E. C. (2005). 23S rRNA base pair 2057–2611 determines ketolide susceptibility and fitness cost of the macrolide resistance mutation 2058A →G. *Proc. Natl Acad. Sci. USA*, **102**, 5180–5185.
15. Pyetan, E., Baram, D., Auerbach-Nevo, T. & Yonath, A. (2007). Chemical parameters influencing fine-tuning in the binding of macrolide antibiotics to the ribosomal tunnel. *Pure Appl. Chem.* **79**, 955–968.
16. Ippolito, J. A., Kanyo, Z. F., Wang, D., Franceschi, F. J., Moore, P. B., Steitz, T. A. & Duffy, E. M. (2008). Crystal structure of the oxazolidinone antibiotic linezolid bound to the 50S ribosomal subunit. *J. Med. Chem.* **51**, 3353–3356.
17. Wilson, D. N., Schluenzen, F., Harms, J. M., Starosta, A. L., Connell, S. R. & Fucini, P. (2008). The oxazolidinone antibiotics perturb the ribosomal peptidyl-transferase center and effect tRNA positioning. *Proc. Natl Acad. Sci. USA*, **105**, 13339–13344.
18. Frank, J. & Agrawal, R. (2000). A ratchet-like intersubunit reorganization of the ribosome during translocation. *Nature*, **406**, 318–322.
19. Gao, H., Sengupta, J., Valle, M., Korostelev, A., Eswar, N., Stagg, S. M. *et al.* (2003). Study of the structural dynamics of the *E. coli* 70S ribosome using real-space refinement. *Cell*, **113**, 789–801.
20. Tama, F., Valle, M., Frank, J. & Brooks, C. L. (2003). Dynamic reorganization of the functionally active ribosome explored by normal mode analysis and cryo-electron microscopy. *Proc. Natl Acad. Sci. USA*, **100**, 9319–9323.
21. Sanbonmatsu, K. Y., Joseph, S. & Tung, C. S. (2005). Simulating movement of tRNA into the ribosome during decoding. *Proc. Natl Acad. Sci. USA*, **102**, 15854–15859.
22. Horan, L. & Noller, H. (2007). Intersubunit movement is required for ribosomal translocation. *Proc. Natl Acad. Sci. USA*, **104**, 4881–4885.
23. Korostelev, A., Trakhanov, S., Laurberg, M. & Noller, H. F. (2006). Crystal structure of a 70S ribosome–tRNA complex reveals functional interactions and rearrangements. *Cell*, **126**, 1065–1077.
24. Gabashvili, I. S., Gregory, S. T., Valle, M., Grassucci, R., Worbs, M., Wahl, M. C. *et al.* (2001). The polypeptide tunnel system in the ribosome and its gating in erythromycin resistance mutants of L4 and L22. *Mol. Cell*, **8**, 181–188.
25. Mitra, K., Schaffitzel, C., Fabiola, F., Chapman, M. S., Ban, N. & Frank, J. (2006). Elongation arrest by SecM via a cascade of ribosomal RNA rearrangements. *Mol. Cell*, **22**, 533–543.
26. Moore, P. B. & Steitz, T. A. (2003). The structural basis of large ribosomal subunit function. *Annu. Rev. Biochem.* **72**, 813–850.
27. Klein, D. J., Moore, P. B. & Steitz, T. A. (2004). The roles of ribosomal proteins in the structure assembly, and evolution of the large ribosomal subunit. *J. Mol. Biol.* **340**, 141–177.
28. Schuwirth, B., Borovinskaya, M., Hau, C., Zhang, W., Vila-Sanjurjo, A., Holton, J. & Cate, J. (2005). Structures of the bacterial ribosome at 3.5 Å resolution. *Science*, **310**, 827–834.
29. Selmer, M., Dunham, C. M., Murphy, F. V., Weixlbaumer, A., Petry, S., Kelley, A. C. *et al.* (2006). Structure of the 70S ribosome complexed with mRNA and tRNA. *Science*, **313**, 1935–1942.
30. Harms, J. M., Wilson, D. N., Schluenzen, F., Connell, S. R., Stachelhaus, T., Zaborowska, Z. *et al.* (2008). Translational regulation via L11: molecular switches on the ribosome turned on and off by thiostrepton and micrococcin. *Mol. Cell*, **30**, 26–38.
31. Wang, Y., Rader, A. J., Bahar, I. & Jernigan, R. (2004). Global ribosome motions revealed with elastic network model. *J. Struct. Biol.* **147**, 302–314.
32. Gohlke, H. & Thorpe, M. F. (2006). A natural coarse graining for simulating large biomolecular motion. *Biophys. J.* **91**, 2115–2120.
33. Petrone, P. M., Snow, C. D., Lucent, D. & Pande, V. S. (2008). Side-chain recognition and gating in the ribosome exit tunnel. *Proc. Natl Acad. Sci. USA*, **105**, 16549–16554.
34. Jacobs, D. J. (1998). Generic rigidity in three-dimensional bond-bending networks. *J. Phys. A Math. Gen.* **31**, 6653–6668.
35. Jacobs, D. J., Rader, A. J., Kuhn, L. A. & Thorpe, M. F. (2001). Protein flexibility predictions using graph theory. *Proteins*, **44**, 150–165.
36. Thorpe, M. F., Lei, M., Rader, A. J., Jacobs, D. J. & Kuhn, L. A. (2001). Protein flexibility and dynamics using constraint theory. *J. Mol. Graphics Modell.* **19**, 60–69.
37. Jacobs, D. J. & Thorpe, M. F. (1995). Generic rigidity percolation: the pebble game. *Phys. Rev. Lett.* **75**, 4051–4054.
38. Gohlke, H., Kuhn, L. A. & Case, D. A. (2004). Change in protein flexibility upon complex formation: analysis of Ras–Raf using molecular dynamics and a molecular framework approach. *Proteins*, **56**, 322–337.
39. Rader, A. J., Hespenheide, B. M., Kuhn, L. A. & Thorpe, M. F. (2002). Protein unfolding: rigidity lost. *Proc. Natl Acad. Sci. USA*, **99**, 3540–3545.
40. Wells, S., Menor, S., Hespenheide, B. & Thorpe, M. F. (2005). Constrained geometric simulation of diffusive motion in proteins. *Phys. Biol.* **2**, 127–136.
41. Ahmed, A. & Gohlke, H. (2006). Multiscale modeling of macromolecular conformational changes combining concepts from rigidity and elastic network theory. *Proteins*, **63**, 1038–1051.
42. Fulle, S. & Gohlke, H. (2008). Analysing the flexibility of RNA structures by constraint counting. *Biophys. J.* **94**, 4202–4219.
43. Harms, J., Schluenzen, F., Zarivach, R., Bashan, A., Gat, S., Agmon, I. *et al.* (2001). High resolution structure of the large ribosomal subunit from a mesophilic eubacterium. *Cell*, **107**, 679–688.
44. Voss, N. R., Gerstein, M., Steitz, T. A. & Moore, P. B. (2006). The geometry of the ribosomal polypeptide exit tunnel. *J. Mol. Biol.* **360**, 893–906.

45. Yusupov, M., Yusupova, G., Baucom, A., Lieberman, K., Earnest, T., Cate, J. H. D. & Noller, H. (2001). Crystal structure of the ribosome at 5.5 Å resolution. *Science*, **292**, 883–896.
46. Ban, N., Nissen, P., Hansen, J., Moore, P. B. & Steitz, T. A. (2000). The complete atomic structure of the large ribosomal subunit at 2.4 Å resolution. *Science*, **289**, 905–920.
47. Tu, D., Blaha, G., Moore, P. & Steitz, T. (2005). Structures of MLS_BK antibiotics bound to mutated large ribosomal subunits provide a structural explanation for resistance. *Cell*, **121**, 257–270.
48. Hansen, J., Ippolito, J., Ban, N., Nissen, P., Moore, P. & Steitz, T. (2002). The structures of four macrolide antibiotics bound to the large ribosomal subunit. *Mol. Cell*, **10**, 117–128.
49. Hansen, J. L., Moore, P. B. & Steitz, T. A. (2003). Structures of five antibiotics bound at the peptidyl transferase center of the large ribosomal subunit. *J. Mol. Biol.* **330**, 1061–1075.
50. Bashan, A., Agmon, I., Zarivach, R., Schluenzen, F., Harms, J., Berisio, R. *et al.* (2003). Structural basis of the ribosomal machinery for peptide bond formation, translocation, and nascent chain progression. *Mol. Cell*, **11**, 91–102.
51. Steitz, T. (2008). A structural understanding of the dynamic ribosome machine. *Nat. Rev. Mol. Cell Biol.* **9**, 242–253.
52. Lu, J. & Deutsch, C. (2005). Folding zones inside the ribosomal exit tunnel. *Nat. Struct. Mol. Biol.* **12**, 1123–1129.
53. Ziv, G., Haran, G. & Thirumalai, D. (2005). Ribosome exit tunnel can entropically stabilize α-helices. *Proc. Natl Acad. Sci. USA*, **102**, 18956–18961.
54. Kirmizialtin, S., Ganesan, V. & Makarov, D. E. (2004). Translocation of a beta-hairpin-forming peptide through a cylindrical tunnel. *J. Chem. Phys.* **121**, 10268–10277.
55. Tenson, T. & Ehrenberg, M. (2002). Regulatory nascent peptides in the ribosomal tunnel. *Cell*, **108**, 591–594.
56. Sarker, S. & Oliver, D. (2002). Critical regions of secM that control its translation and secretion and promote secretion-specific secA regulation. *J. Bacteriol.* **184**, 2360–2369.
57. Woolhead, C. A., Johnson, A. E. & Bernstein, H. D. (2006). Translation arrest requires two-way communication between a nascent polypeptide and the ribosome. *Mol. Cell*, **22**, 587–598.
58. Mitra, K. & Frank, J. (2006). Ribosome dynamics: insights from atomic structure modeling into cryo-electron microscopy maps. *Annu. Rev. Biophys. Biomol. Struct.* **35**, 299–317.
59. Lawrence, M. G., Lindahl, L. & Zengel, J. M. (2008). Effects on translation pausing of alterations in protein and RNA components of the ribosome exit tunnel. *J. Bacteriol.* **190**, 5862–5869.
60. Unge, J., Berg, A., Al-Kharadaghi, S., Nikulin, A., Nikonov, S., Davydova, N. *et al.* (1998). The crystal structure of ribosomal protein L22 from *Thermus thermophilus*: insights into the mechanism of erythromycin resistance. *Structure*, **6**, 1577–1586.
61. Sitharam, M. & Agbandje-Mckenna, M. (2006). Modeling virus self-assembly pathways: avoiding dynamics using geometric constraint decomposition. *J. Comput. Biol.* **13**, 1232–1265.
62. Kramer, G., Rauch, T., Rist, W., Vorderwulbecke, S., Patzelt, H., Schulze-Specking, A. *et al.* (2002). L23 protein functions as a chaperone docking site on the ribosome. *Nature*, **419**, 171–174.
63. Baram, D., Pyetan, E., Sittner, A., Auerbach-Nevo, T., Bashan, A. & Yonath, A. (2005). Structure of trigger factor binding domain in biologically homologous complex with eubacterial ribosome reveals its chaperone action. *Proc. Natl Acad. Sci. USA*, **102**, 12017–12022.
64. Gu, S. Q., Peske, F., Wieden, H. J., Rodnina, M. V. & Wintermeyer, W. (2003). The signal recognition particle binds to protein L23 at the peptide exit of the *Escherichia coli* ribosome. *RNA*, **9**, 566–573.
65. Bornemann, T., Jöckel, J., Rodnina, M. V. & Wintermeyer, W. (2008). Signal sequence-independent membrane targeting of ribosomes containing short nascent peptides within the exit tunnel. *Nat. Struct. Mol. Biol.* **15**, 494–499.
66. Baram, D. & Yonath, A. (2005). From peptide-bond formation to cotranslational folding: dynamic, regulatory and evolutionary aspects. *FEBS Lett.* **579**, 948–954.
67. Dresios, J., Derkatch, I. L., Liebman, S. W. & Synetos, D. (2000). Yeast ribosomal protein L24 affects the kinetics of protein synthesis and ribosomal protein L39 improves translational accuracy, while mutants lacking both remain viable. *Biochemistry*, **39**, 7236–7244.
68. Dresios, J., Panopoulos, P. & Synetos, D. (2006). Eukaryotic ribosomal proteins lacking a eubacterial counterpart: important players in ribosomal function. *Mol. Microbiol.* **59**, 1651–1663.
69. Spahn, C. M. & Prescott, C. D. (1996). Throwing a spanner in the works: antibiotics and the translation apparatus. *J. Mol. Med.* **74**, 423–439.
70. Yonath, A. (2005). Ribosomal crystallography: peptide bond formation, chaperone assistance and antibiotics activity. *Mol. Cells*, **20**, 1–16.
71. Poehlsgaard, J. & Douthwaite, S. (2005). The bacterial ribosome as target for antibiotics. *Nat. Rev. Microbiol.* **3**, 870–881.
72. Hansen, J., Schmeing, M., Moore, P. & Steitz, T. (2002). Structural insights into peptide bond formation. *Proc. Natl Acad. Sci. USA*, **99**, 11670–11675.
73. Schmeing, T. M., Seila, A. C., Hansen, J. L., Freeborn, B., Soukup, J. K., Scaringe, S. A. *et al.* (2002). A pre-translocational intermediate in protein synthesis observed in crystals of enzymatically active 50S subunits. *Nat. Struct. Biol.* **9**, 225–230.
74. Weixlbaumer, A., Petry, S., Dunham, C., Selmer, M., Kelley, A. & Ramakrishnan, V. (2007). Crystal structure of the ribosome recycling factor bound to the ribosome. *Nat. Struct. Mol. Biol.* **14**, 733–737.
75. Schuwirth, B., Day, J. M., Hau, C. W., Janssen, G. R., Dahlberg, A. E., Cate, J. H. & Vila-Sanjurjo, A. (2006). Structural analysis of kasugamycin inhibition of translation. *Nat. Struct. Mol. Biol.* **13**, 879–886.
76. Borovinskaya, M., Pai, R., Zhang, W., Schuwirth, B., Holton, J., Hirokawa, G. *et al.* (2007). Structural basis for aminoglycoside inhibition of bacterial ribosome recycling. *Nat. Struct. Mol. Biol.* **14**, 727–732.
77. Vazquez-Laslop, N., Thum, C. & Mankin, A. S. (2008). Molecular mechanism of drug-dependent ribosome stalling. *Cell*, **30**, 190–202.
78. Auerbach, T., Bashan, A. & Yonath, A. (2004). Ribosomal antibiotics: structural basis for resistance, synergism and selectivity. *Trends Biotechnol.* **22**, 570–576.
79. Yonath, A. & Bashan, A. (2004). Ribosomal crystallography: initiation, peptide bond formation, and amino acid polymerization are hampered by antibiotics. *Annu. Rev. Microbiol.* **58**, 233–251.
80. Mankin, A. S. & Garrett, R. A. (1991). Chloramphenicol resistance mutations in the single 23S rRNA gene

of the archaeon *Halobacterium halobium*. *J. Bacteriol.* **173**, 3559–3563.
81. Sanz, J. L., Marín, I., Ureña, D. & Amils, R. (1993). Functional analysis of seven ribosomal systems from extremely halophilic archaea. *Can. J. Microbiol.* **39**, 311–317.
82. Schluenzen, F., Harms, J. M., Franceschi, F., Hansen, H. A., Bartels, H., Zarivach, R. & Yonath, A. (2003). Structural basis for the antibiotic activity of ketolides and azalides. *Structure*, **11**, 329–338.
83. Blaha, G., Gürel, G., Schroeder, S. J., Moore, P. B. & Steitz, T. A. (2008). Mutations outside the anisomycin-binding site can make ribosomes drug-resistant. *J. Mol. Biol.* **379**, 505–519.
84. Davidovich, C., Bashan, A., Auerbach-Nevo, T., Yaggie, R. D., Gontarek, R. R. & Yonath, A. (2007). Induced-fit tightens pleuromutilins binding to ribosomes and remote interactions enable their selectivity. *Proc. Natl Acad. Sci. USA*, **104**, 4291–4296.
85. Wen, J. D., Lancaster, L., Hodges, C., Zeri, A. C., Yoshimura, S., Noller, H. *et al.* (2008). Following translation by single ribosomes one codon at a time. *Nature*, **452**, 598–603.
86. Radestock, S. & Gohlke, H. (2008). Exploiting the link between protein rigidity and thermostability for data-driven protein engineering. *Eng. Life Sci.* **8**, 507–522.
87. Fuller, R. B. (1960). *Portfolio and Art News Annual*, vol. 4, pp. 112–127, 144, 146, Art Foundation Press, New York.
88. Ingber, D. (2003). Tensegrity: I. Cell structure and hierarchical systems biology. *J. Cell Sci.* **116**, 1157–1173.
89. Giuseppe, Z. & Guerra, C. (2003). Is tensegrity a unifying concept of protein folds? *FEBS Lett.* **534**, 7–10.
90. Draper, D. E. (2004). A guide to ions and RNA structure. *RNA*, **3**, 335–343.
91. Case, D. A., Cheatham, T. E., Darden, T., Gohlke, H., Luo, R., Merz, K. M. *et al.* (2005). The Amber biomolecular simulation programs. *J. Comput. Chem.* **26**, 1668–1688.
92. Whiteley, W. (2005). Counting out to the flexibility of molecules. *Phys. Biol.* **2**, 116–126.
93. Perederina, A., Nevskaya, N., Nikonov, O., Nikulin, A., Dumas, P., Yao, M. *et al.* (2002). Detailed analysis of RNA–protein interactions within the bacterial ribosomal protein L5/5S rRNA complex. *RNA*, **8**, 1548–1557.